

**Electronic Supplementary Information (ESI) for Journal of Materials Chemistry C**

**Benefits of surfactant effects on quantum efficiency  
enhancement and temperature sensing behavior of NaBiF<sub>4</sub>  
upconversion nanoparticles**

Pengpeng Lei,<sup>a,b</sup> Ran An,<sup>a</sup> Xuesong Zhai,<sup>d</sup> Shuang Yao,<sup>a</sup> Lile Dong,<sup>a,c</sup> Xia Xu,<sup>a,b</sup>

Kaimin Du,<sup>a,c</sup> Manli Zhang,<sup>a,c</sup> Jing Feng,<sup>a,\*</sup> and Hongjie Zhang<sup>a,\*</sup>

<sup>a</sup> State Key Laboratory of Rare Earth Resource Utilization, Changchun Institute of Applied Chemistry, Chinese Academy of Sciences, 5625 Renmin Street, Changchun 130022, China

<sup>b</sup> University of Chinese Academy of Sciences, Beijing 100049, China

<sup>c</sup> University of Science and Technology of China, Hefei 230026, China

<sup>§</sup>School of Materials Engineering, Yancheng Institute of Technology, Yancheng 224051, China

\* Corresponding authors. Tel.: +86 431 85262127; fax: +86 431 85698041.

E-mail addresses: fengj@ciac.ac.cn (J. Feng), hongjie@ciac.ac.cn (H. Zhang).

**KEYWORDS:** NaBiF<sub>4</sub>, upconversion luminescence, polyacrylic acid, quantum efficiency, temperature sensing

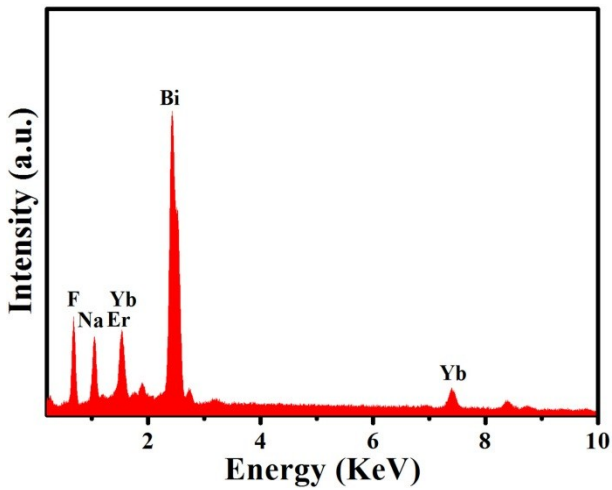


**Fig. S1** X-ray Energy-dispersive (EDX) spectroscopy of  $\text{NaBiF}_4:\text{Yb}^{3+}/\text{Er}^{3+}$  UCNPs.

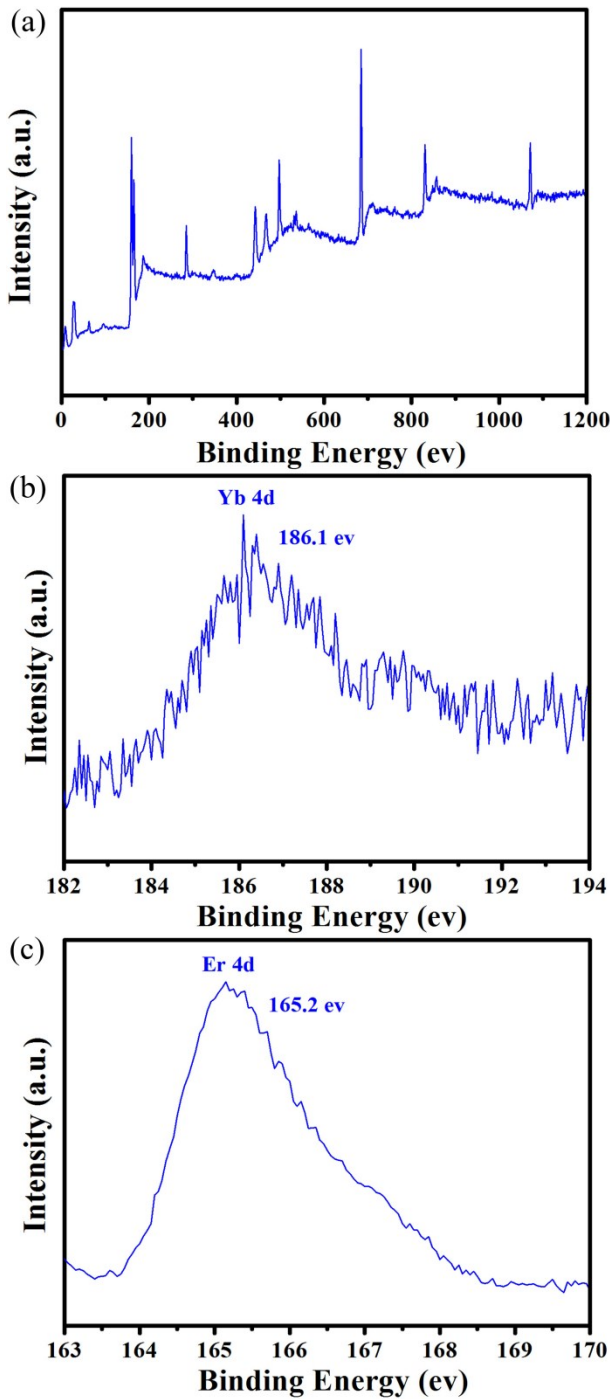


**Fig. S2** X-ray photoelectron spectroscopy (XPS) survey spectra of  $\text{NaBiF}_4:\text{Yb}^{3+}/\text{Er}^{3+}$  UCNPs. (a) survey, (b) Yb 4d, and (c ) Er 4d.

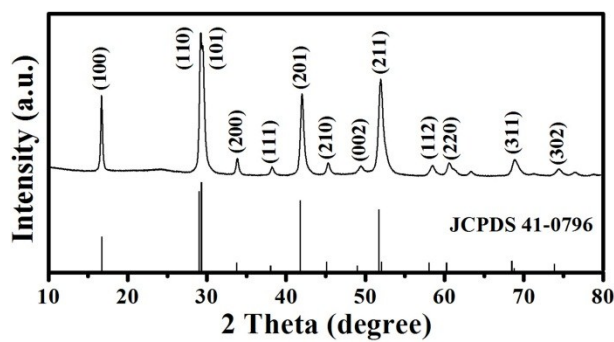


**Fig. S3** XRD pattern of PAA-modified  $\text{NaBiF}_4\text{:Yb}^{3+}/\text{Er}^{3+}$  UCNPs.

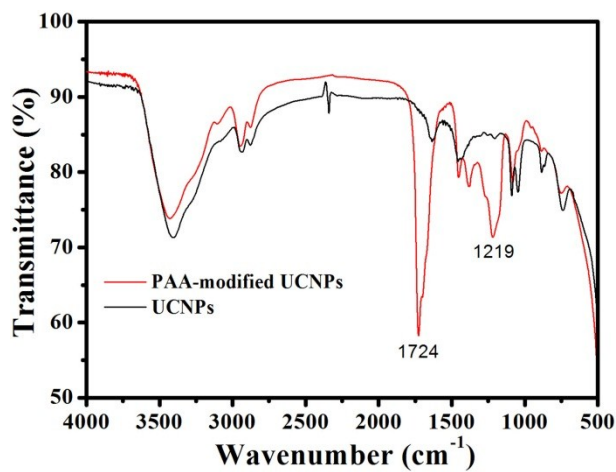


**Fig. S4** FT-IR spectra of  $\text{NaBiF}_4:\text{Yb}^{3+}/\text{Er}^{3+}$  and PAA-modified  $\text{NaBiF}_4:\text{Yb}^{3+}/\text{Er}^{3+}$  UCNPs.

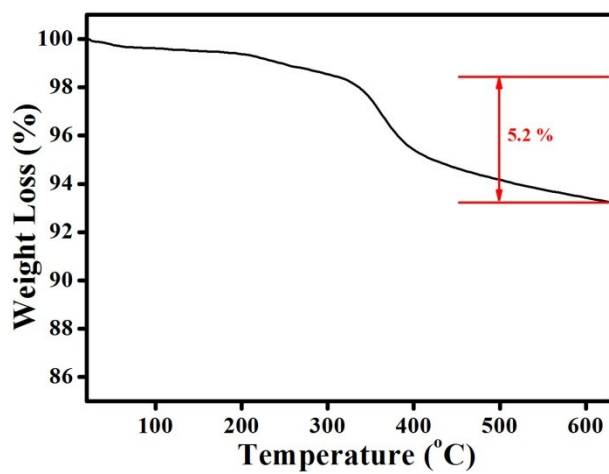


**Fig. S5** Thermo-gravimetric (TG) analysis of PAA-modified NaBiF<sub>4</sub>:Yb<sup>3+</sup>/Er<sup>3+</sup> UCNPs.

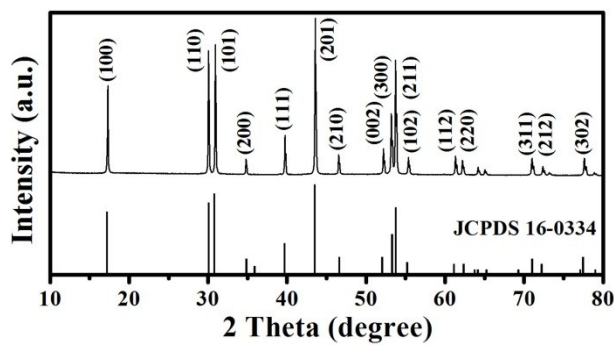


**Fig. S6** XRD pattern of NaYF<sub>4</sub>:Yb<sup>3+</sup>/Er<sup>3+</sup> UCNPs.

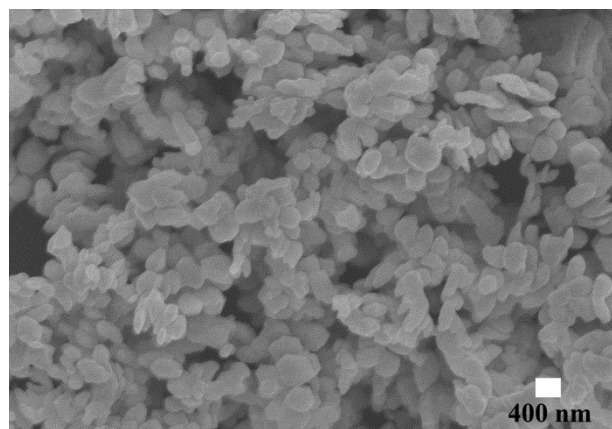


**Fig. S7** SEM image of NaYF<sub>4</sub>:Yb<sup>3+</sup>/Er<sup>3+</sup> UCNPs.

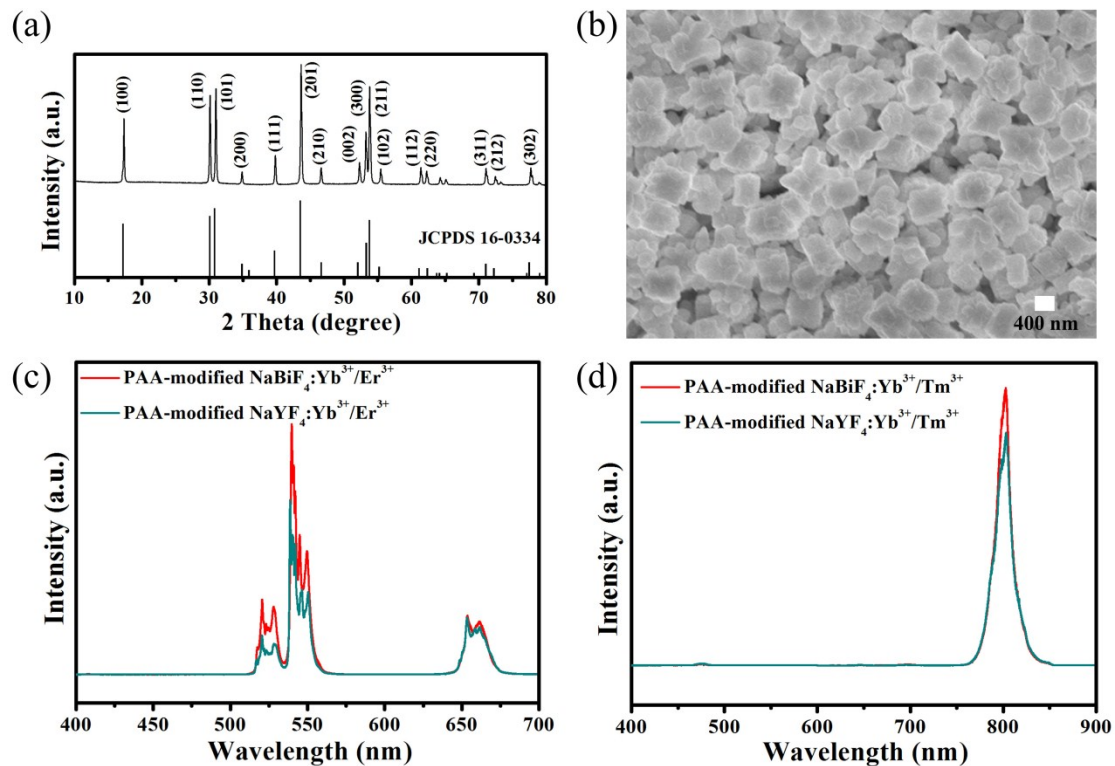


**Fig. S8** XRD pattern (a) and SEM image (b) of PAA-modified  $\text{NaYF}_4:\text{Yb}^{3+}/\text{Er}^{3+}$  UCNPs. UCL spectra of (c) PAA-modified  $\text{NaBiF}_4:\text{Yb}^{3+}/\text{Er}^{3+}$  and PAA-modified  $\text{NaYF}_4:\text{Yb}^{3+}/\text{Er}^{3+}$  and (d) PAA-modified  $\text{NaBiF}_4:\text{Yb}^{3+}/\text{Tm}^{3+}$  and PAA-modified  $\text{NaYF}_4:\text{Yb}^{3+}/\text{Tm}^3$  under 980 nm NIR excitation ( $11.3 \text{ W/cm}^2$ ).

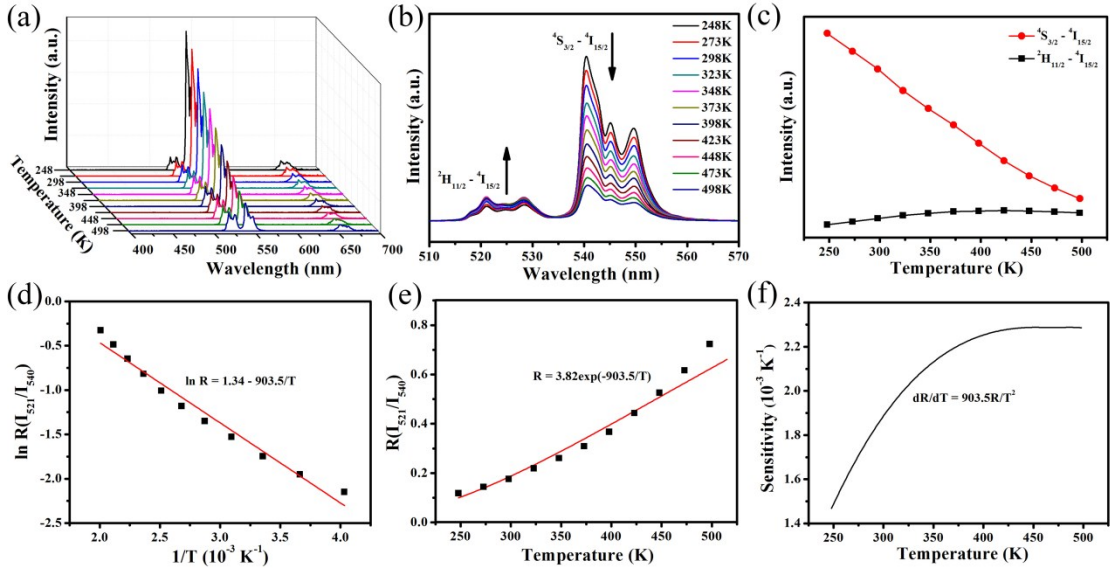


**Fig. S9** (a) Temperature dependent UCL spectra of  $\text{NaBiF}_4:\text{Yb}^{3+}/\text{Er}^{3+}$  UCNP at various temperatures under 980 nm excitation ( $21.2 \text{ W/cm}^2$ ). (b) The green UCL spectra of  $\text{Er}^{3+}$  from  $^2\text{H}_{11/2}$  and  $^4\text{S}_{3/2}$  levels to the  $^4\text{I}_{15/2}$  level at different temperature. (c) The integrated luminescence intensity plots of  $\text{Er}^{3+}$  at 521 ( $^2\text{H}_{11/2} - ^4\text{I}_{15/2}$ ) and 540 nm ( $^4\text{S}_{3/2} - ^4\text{I}_{15/2}$ ). (d) Monolog plot of  $R$  ( $I_{521}/I_{540}$ ) as a function of inverse absolute temperature. (e)  $R$  ( $I_{521}/I_{540}$ ) relative to the absolute temperature. (f) The sensing sensitivity as a function of the absolute temperature.